Laser-Doppler Measurements of Impinging Jet Flows Through a Crossflow

by

J.M.M. Barata[(1)] and D.F.G. Durão[(2)]

[(1)]Universidade da Beira Interior
Aerospace Sciences Department
Rua Marquês d'Ávila e Bolama
6201-001 Covilhã, Portugal
Email: jbarata@ubi.pt

[(2)]Instituto Superior Técnico
Mechanical Engineering Department
Av. Rovisco Pais, 1049-001 Lisboa, Portugal
Email: ddurao@dem.ist.utl.pt

ABSTRACT

The flowfield resulting from the impingement of a single axisymmetric jet against a wall after penetrating a confined cross-flow has been studied experimentally using laser-Doppler anemometry. For sufficiently high jet velocities and small distances between the jet exit and the ground plane to produce impingement, two regions of the flow are seen to be of particular interest: the impinging region and the ground vortex due to the interaction between the upstream wall jet and the crossflow. The latter consists of a vortical structure that wraps around the impinging jet like a scarf and should develop further downstream through a pair of streamwise vortices. The present work reports a study aimed at characterizing the influence of the jet-to-crossflow velocity ratio on the structure of the ground vortex. The experiments were performed for Reynolds numbers based on the jet-exit conditions of between 60,000 and 105,000 corresponding to jet-to-crossflow velocity ratios from 30 to 73 and for an impinging height of 5 jet diameters. The shape, size and location of the ground vortex were found to be dependent on the velocity ratio, and two different regimes were identified. For the higher velocity ratio regime the downstream wall jet it is not strongly affected by the ground vortex, and the velocity profiles become similar. In both regimes, the crossflow acceleration over the ground vortex was found to be directly connected with the jet exit velocity. This indicates that the influence of the upstream wall jet is not confined to the ground vortex but spreads until the upper wall by a mechanism that needs further investigation.

NOMENCLATURE

D	=	diameter of the jet
H	=	height of crossflow channel
R_e	=	Reynolds number
U	=	mean horizontal velocity component
V	=	mean vertical velocity component
X	=	horizontal coordinate (positive in the direction of cross-flow)
Y	=	vertical coordinate (distance to the ground floor)
Subscripts		
j	=	jet-exit
o	=	crossflow

1. INTRODUCTION

Turbulent jets impinging on flat surfaces through a low-velocity crossflow are typical in impingement cooling applications in industry, as well as of the flow beneath a short/vertical take-off aircraft which is lifting off or landing with zero or small forward momentum. Ground effect may occur and change the lift forces on the aircraft, cause reingestion of exhaust gases into the engine intake and raise fuselage skin temperatures. In this latter application the impingement of each downward-directed jet on the ground results in the formation of a wall jet which flows radially from the impinging point along the ground surface. The interaction of these wall jets with the free stream results in the formation of a ground vortex far upstream of the impinging jet, which has profound implications on the aircraft design (e.g. Barata et al., 1989 and Knowles and Bray, 1991). In addition the collision of the wall jets originates a fountain upwash flow, affecting the forces and moments induced in the aircraft when operating in ground effect. Improved knowledge of impinging flows is therefore necessary to avoid these effects and to be able to model a range of jet-impingement type of applications with practical interest.

This paper presents laser-Doppler measurements of the velocity characteristics of the flow produced by a single round jet discharged through the upper wall of a rectangular water channel of large cross section (.5m x .1m) at right angles to the channel flow and is aimed at characterizing the influence of the jet-to-crossflow velocity ratio on the structure of the ground vortex.

Measurements of the velocity characteristics of normal impinging jets on a flat surface have been reported for single jet configurations for relatively large impingement heights and normally for H/D>10, using either probe and optical techniques, as reviewed for example by Barata (1989) and Araújo et al. (1982). Sugiyama and Usami (1979), Andreopulos and Rodi (1984) and Shayesteh et al. (1985) report hot-wire measurements for ratios H/D greater than 24 and for values of Vj/U/o respectively up to 1.95, 2 and 16. Kamotani and Greber (1974) present results for H/D=12 and Stoy and Ben-Haim (1973) give pitot-tube measurements for values of H/D=3.05 and for jet-to-crossflow velocity ratios up to 6.8. Crabb et al. (1981) report LDV measurements, including those of shear stress, but for values of H/D=12 and for velocity ratios up to 2.3. More recently, Barata et al. (1993) and Barata (1996) provided detailed LDV measurements for a single and multiple jet configurations for jet Reynolds numbers of $6x10^4$ and $1.05x10^5$, a velocity ratio between the jet and the crossflow of 30, and an impinginging height of 5 jet-diameters. The measurements include time-resolved velocity characteristics along the horizontal and vertical directions, and respective correlation's, in planes parallel to the jet nozzle axis. The results are complemented in the present work by a detailed analysis of the ground vortex and its implications in the development of the impinging flows.

The remainder of this paper is presented in four sections. Section 2 describes the experimental configuration and measurement procedure. Section 3 presents the experimental results obtained in vertical plane of symmetry that contains the jet nozzle axis and quantifies the mean and turbulent velocity characteristics of the flow. The main characteristics (location, size, penetration, etc.) of the ground vortex and the influence of the velocity ratio on its development are also specifically analyzed. The final section summarizes the main findings and conclusions of this work.

2. EXPERIMENTAL METHOD

2.1 Flow Configuration

The experiments were carried out in a horizontal water channel, 1.50m long and 0.5m wide, made of Perspex, as described in detail by Barata (1989). The crossflow duct extends 20D upstream and 55D downstream of the jet exit, which is symmetrically located 12.5D from each side wall. The jet unit comprises a nozzle with an area contraction ratio of 16 and a settling chamber 0.56m long, which begins with a flow distributor (with an aperture of 7º) followed by flow straighteners. The uniformity of the crossflow was ensured by straighteners and screens.

The origin of the horizontal (X) and vertical (Y) coordinates is taken at the center of the jet exit in the upper wall of the tunnel: X is positive in the crossflow direction and Y is positive vertically upwards. The present results were obtained at the vertical plane of symmetry for jet exit mean velocities of 3, 4.2, and 6 m/s, giving rise to Reynolds numbers based on jet exit conditions of 60 000, 84 000 and 120 000, respectively. The crossflow velocities used were 0.1, 0.093, and 0.082 m/s, corresponding to velocity ratios between the jet and the crossflow (V_j/U_o) of 30, 45, and 73, respectively.

2.2 Experimental Techniques and Measurement Procedure

The velocity was measured by a dual-beam forward scatter laser velocimeter, which comprised an argon-ion laser (514.5nm; 1W nominal power) and operated in the dual-beam, forward-scatter mode with sensivity of the flow direction provided by light-frequency shifting from acousto-optic modulation (Bragg cells). The calculated half-angle of beam intersection in water was 3.48deg and the dimensions of the measuring volume at e^{-2} intensity, were 2.225 and 0.135mm.

The light scattered by naturally-occurring centers in the water was collected by a lens (focal length of 150 mm) and focused into the pinhole aperture (0.3mm) of a photomultiplier (EMI D136B) with a magnification of 0.76. The output of the photomultiplier was band-pass filtered and the resulting signal processed by a laboratory-built frequency counter. Each measurement is subject to preset validations in the amplitude and time domains and, if valid, is digitized as a floating-point number and transferred to a microcomputer.

The complete LDV system is mounted on a three-dimensional transversing unit, allowing the positioning of the laser-velocimeter control volume within ±0.5mm. The horizontal, U, and vertical, V, mean velocity components and corresponding Reynolds shear stresses were determined from measurements with the laser beams in the horizontal and vertical planes and at ±45deg in the way described, for example, by Melling and Whitelaw (1975). In order to measure the vertical components in near wall regions, the transmitting optics were inclined by half angle of beam intersection, and the scattered light was collected off-axis. Measurements could then be obtained up to 2mm from the ground plate without a significant deterioration of the Doppler signals. Results obtained 20mm above the ground plate with both the on-axis and the off-axis arrangements have shown a close agreement, within the precision of the equipment.

Errors incurred in the measurement of velocity by displacement and distortion of the measuring volume due to refraction on the duct walls and change in the refractive index were found to be negligibly small and within the accuracy of the measuring equipment. Non-turbulent Doppler broadening errors due to gradients of mean velocity across the measuring volume (e.g., Durst et al., 1981) may affect essentially the variance of the velocity fluctuations, but for the present experimental conditions are of the order of $10^{-4}V_j^2$ and, therefore, sufficiently small for their effect to be neglected. The largest statistical (random) errors derived form populations of , at least, 10000 velocity values were of 0.5 and 3%, respectively for the mean and the variance values, according to the analysis recommended by Yanta and Smith (1978) for a 95% confidence interval.
Systematic errors incurred in the measurements of Reynolds shear stresses can arise from lack of accuracy in the orientation angle on the normal to the anemometer fringe pattern, as shown by Melling and Whitelaw (1975), and can be particularly large in the vicinity of the zones characterized by zero shear stress: for the present experimental conditions the largest errors are expected to be smaller than 2.5%.

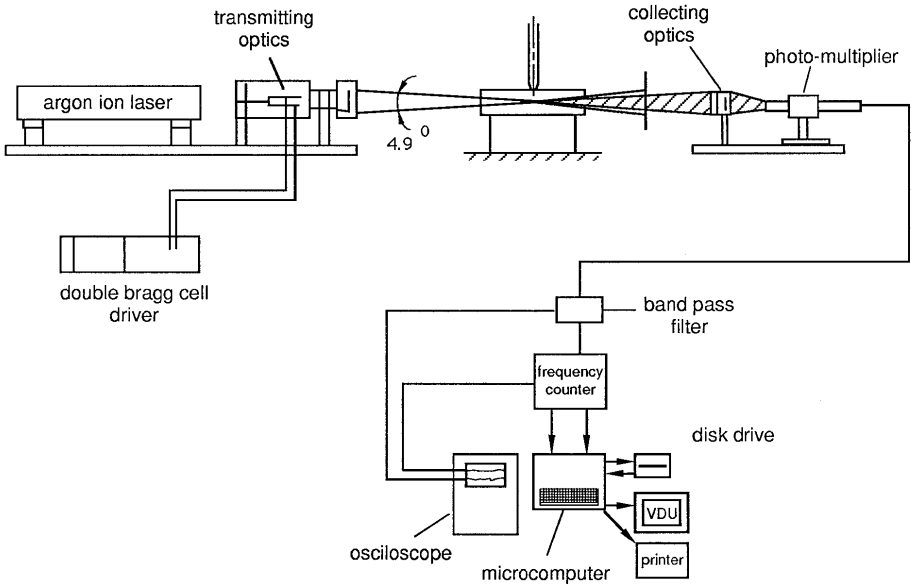

Fig. 1. Diagram of the LDV system

3. RESULTS

Prior to the detailed measurements extensive visualization studies of the flow were performed to guide the choice of the measurement locations and to provide a qualitative picture of the flow (see Barata, 1989). The results have identified an initial potential-core jet region, where the flow characteristics are identical to those of a free jet, and the impingement region, characterized by considerable deflection of the jet after being slightly bent downstream by the pressure difference established across the jet. The deflected jet becomes almost parallel to the ground plate and exhibits a behavior similar to that of a radial wall jet where the upstream effects of interaction due to impingement are no longer important. The upstream wall jet interacts with the crossflow and forms a vortex close to the ground plate, which wraps around the impinging jet like a scarf. As a result, two streamwise counter-rotating vortices develop side-to-side and decay further downstream of the impinging zone (figure 2). The flow is similar to the horseshoe structure known to be generated by the deflection of a boundary layer by a solid obstacle (e.g. Baker, 1981), but is different from the vortex pair known to exist in a "bent-over" jet in a crossflow far from the ground (e.g. Andreopoulos and Rodi, 1984).

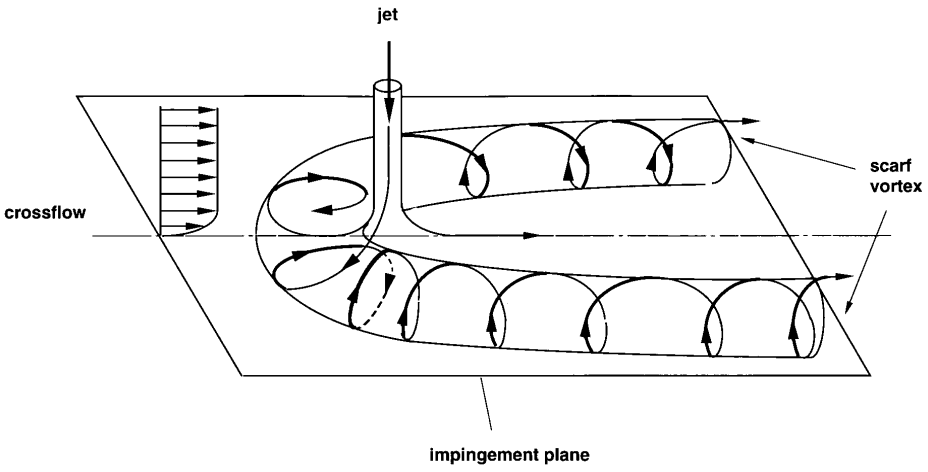

Fig. 2. Jet impinging on a flat surface through a low-velocity crossflow.

The following paragraphs examine the experimental results obtained in vertical plane of symmetry that contains the jet nozzle axis and quantifies the mean and turbulent velocity characteristics of the flow.

Fig. 3 shows the measured velocity fields in the vertical plane of symmetry V_j for velocity ratios (V_j/U_o) of 30 and 45. The mean velocity components were fed into Tecplot 7.5 to represent the velocity vectors and the streamlines. This figure clearly identifies the ground vortex mentioned before, due to the interaction of the crossflow with the upstream wall jet. The deflection of the impinging jet by the crossflow decreases as the jet velocity is increased, and is identified by the location of the impinging point: about X/D=0.2 for V_j/U_o=30 and at about X/D=0.1 for V_j/U_o=45. The ground vortex moves upstream when the jet-to-crossflow velocity increases: the center is located at X/D=-5.6 for V_j/U_o=30 and at X/D=-7.2 for V_j/U_o=45. Nevertheless, the vertical coordinate of the center of the vortex is about Y/D=1.08 for the two velocity ratios. The size is reduced when V_j/U_o increases: the length is 8.8D for V_j/U_o=30 and 7.1D for V_j/U_o=45, while the height is 2.95 and 2.55, respectively. This figure also reveals a most important feature that characterizes two different regimes: in figure 3a) for the smaller velocity ratio the ground vortex is attached to the impinging jet, while for the larger velocity ratio (figure 3b) is completely detached. This has profound implications in the flow development and explains some features never explained before as, for example, the apparent "lifting" of the downstream wall jet that can be observed in figure 3a. In the next paragraphs and with the additional help of figure 4 this subject is developed.

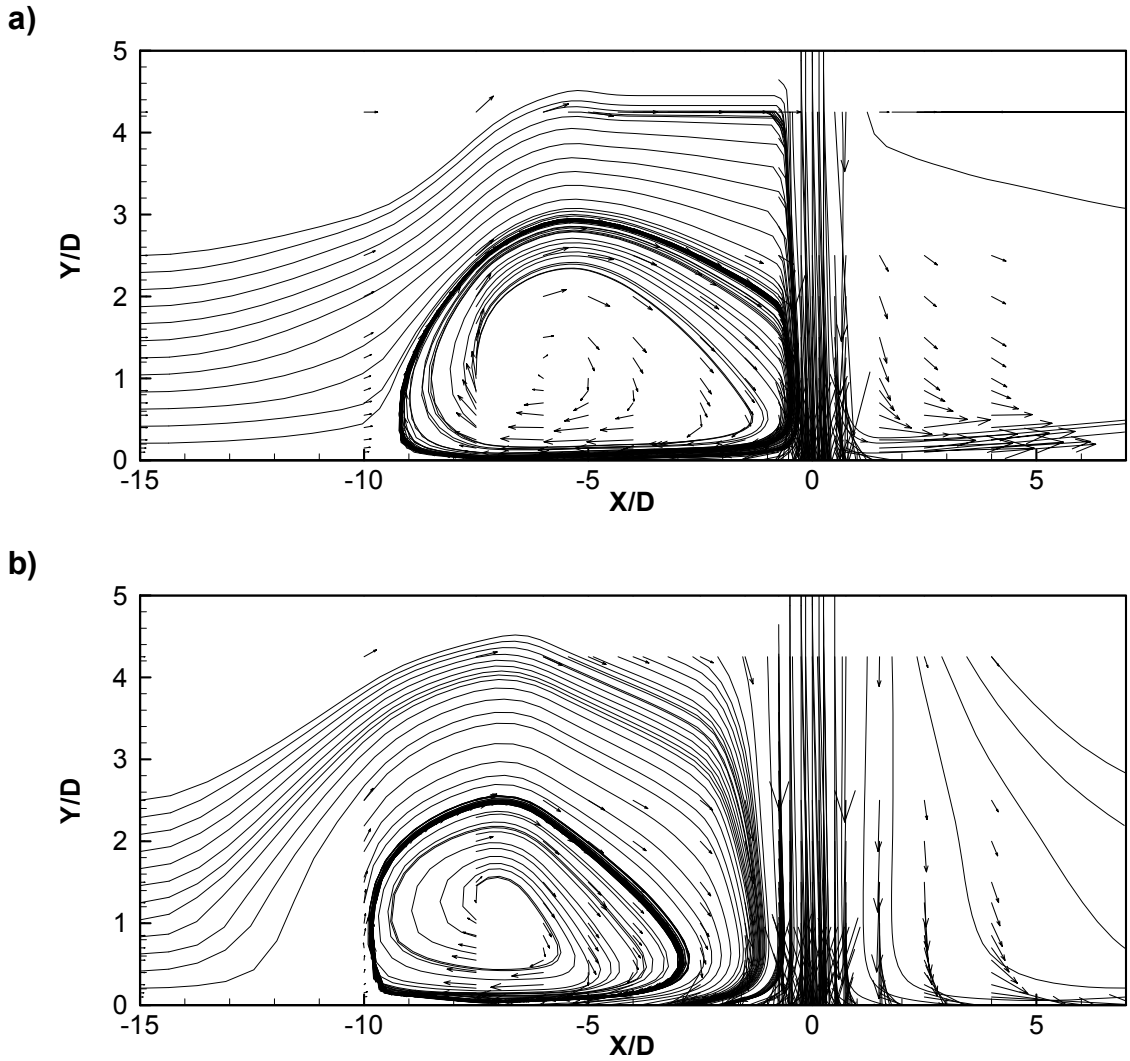

Fig. 3. Measured mean velocity characteristics in the vertical plane of symmetry for two different jet-to-crossflow velocity ratios: a) V_j/U_o=30; b) V_j/U_o=45.

Figure 4 shows typical measured vertical profiles of the mean velocity components U and V and extends the information of the previous figure up to velocity ratios V_j/U_o=73. The above mentioned lifting of the

downstream wall jet is also noted in this figure by the positive (i.e. upwards) mean vertical velocities that correspond to a maximum inclination of 3.8º at X/D=2.5 for V_j/U_o=30. This is associated with the interference of the ground vortex in the upstream edge of the impinging jet that feeds it with fluid, but with low momentum. Additionally, the ground vortex is blocking the passage of the crossflow fluid in the region near to the wall ($0<Y/D<2$), and as a result the downstream wall jet grows at an abnormal rate near the impinging zone and the vertical velocity component increases. So, there is no separation, but only an abnormal deficit of momentum in downstream side of the impinging jet over the wall jet. For higher velocity ratios this effect it is not significant because the ground vortex is detached from the jet and is smaller in height, reducing this effect of blockage. As a consequence, the crossflow is deflected over the ground vortex but downstream the impinging jet is more aligned with the wall jet that will develop as the usual radial wall jet (e.g. Rajaratnam, 1976). The present results clearly identify two different regimes for impinging jets through a low velocity crossflow: one with "contact" between the ground vortex and the impinging jet and another with the vortex detached upstream the impinging zone. These two velocity ratios regime are also identified by the similarity of the normalized velocity profiles observed in figure 4 for V_j/U_o=45 and V_j/U_o=73.

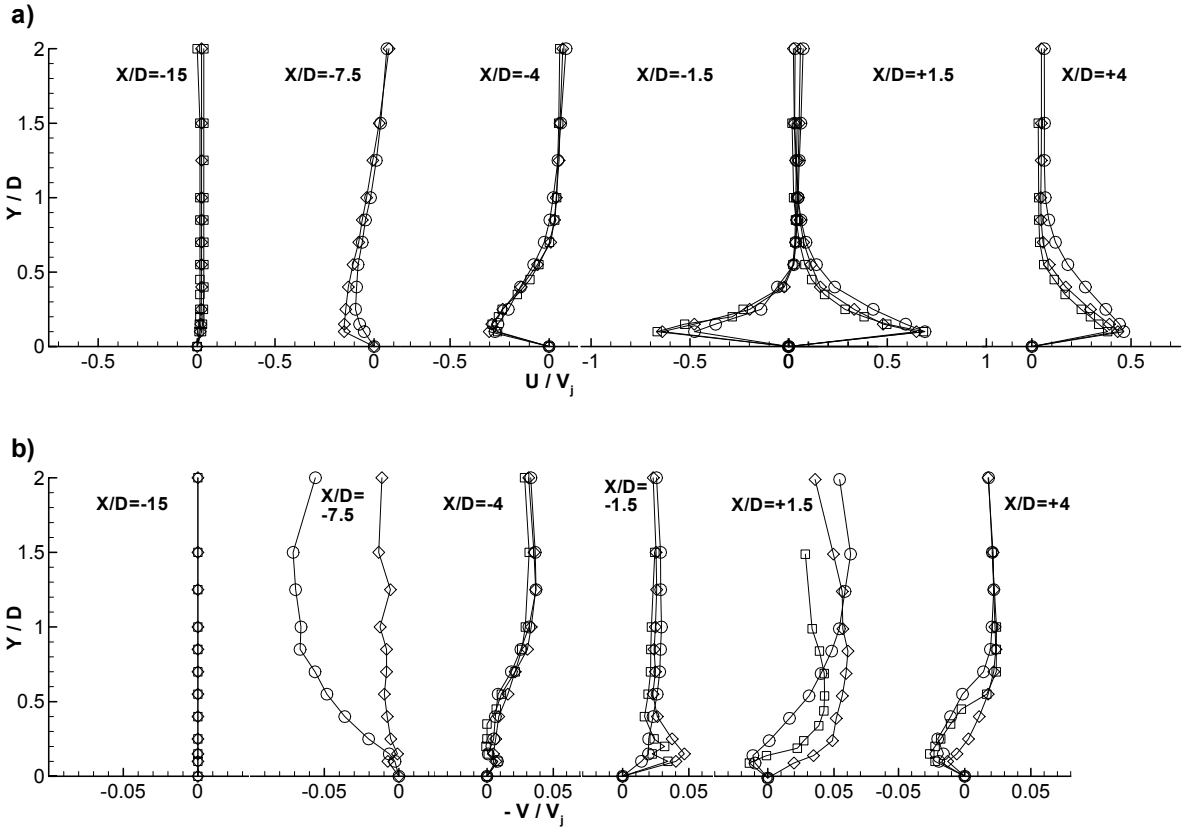

Fig. 4. Vertical profiles of mean velocity characteristics as a function of the jet-to-crossflow velocity ratio.
a) Axial velocity component, U/V_j
b) Vertical velocity component, V/V_j
Key: (O) V_j/U_o=30; (◊) V_j/U_o=45; ( ) V_j/U_o=73.

Figures 5 and 6 show contours of measured turbulent characteristics for V_j/U_o=30 and 45 and indicates two regions of intense velocity fluctuations: the shear layer surrounding the impinging jet and the impinging zone itself (including the bottom part of the ground vortex). Both are located where the mean velocity gradients occur and are associated with near-Gaussian velocity probability distributions suggesting the absence of discrete frequency oscillations. The influence of the velocity ratio V_j/U_o upon the shape of the contours is small, but the maxima of the stresses increase as V_j/U_o increases. Nevertheless, there are evidences of the two different flow regimes mentioned above: one is characteristic of the smaller velocity ratio and is identified by high gradients of the velocity fluctuations near the upstream side of the impinging jet, while the other for higher velocity ratios is characterized by a more symmetric distribution and smaller gradients of turbulent quantities.

The contours of the shear stress *u'v'* (figures 7a and b) quantify the turbulent diffusion along the impinging and wall jets. The sign of the shear stress is consistent with the direction of the mean flow, with near zero values near the center of the impinging jet. The shear stress is positive along the downstream edge of the impinging jet and shows that faster moving elements of jet fluid tend to move outwards into the wake of the jet. Similarly, the shear stress is negative along the upstream edge of the jet because the faster moving elements of jet fluid are associated with negative horizontal velocity fluctuations. Along the wall jets a similar analysis holds, and the shear stress is positive upstream the jet exit and negative otherwise. The results also show that away from the impinging zone the sign of the shear stress *u'v'* is related to the sign of the shear strain in accordance with a turbulent viscosity hypothesis (see Barata et al., 1993). It is also noted the effect of the velocity ratio regime in the upstream side of the impinging jet where high values of the turbulent shear stress (larger than 15 $x10^3/V_j^2$ in absolute value) occur together with high shear stress gradients. This effect is even more pronounced near the impinging zone where the thin shear layer approximation is no longer valid.

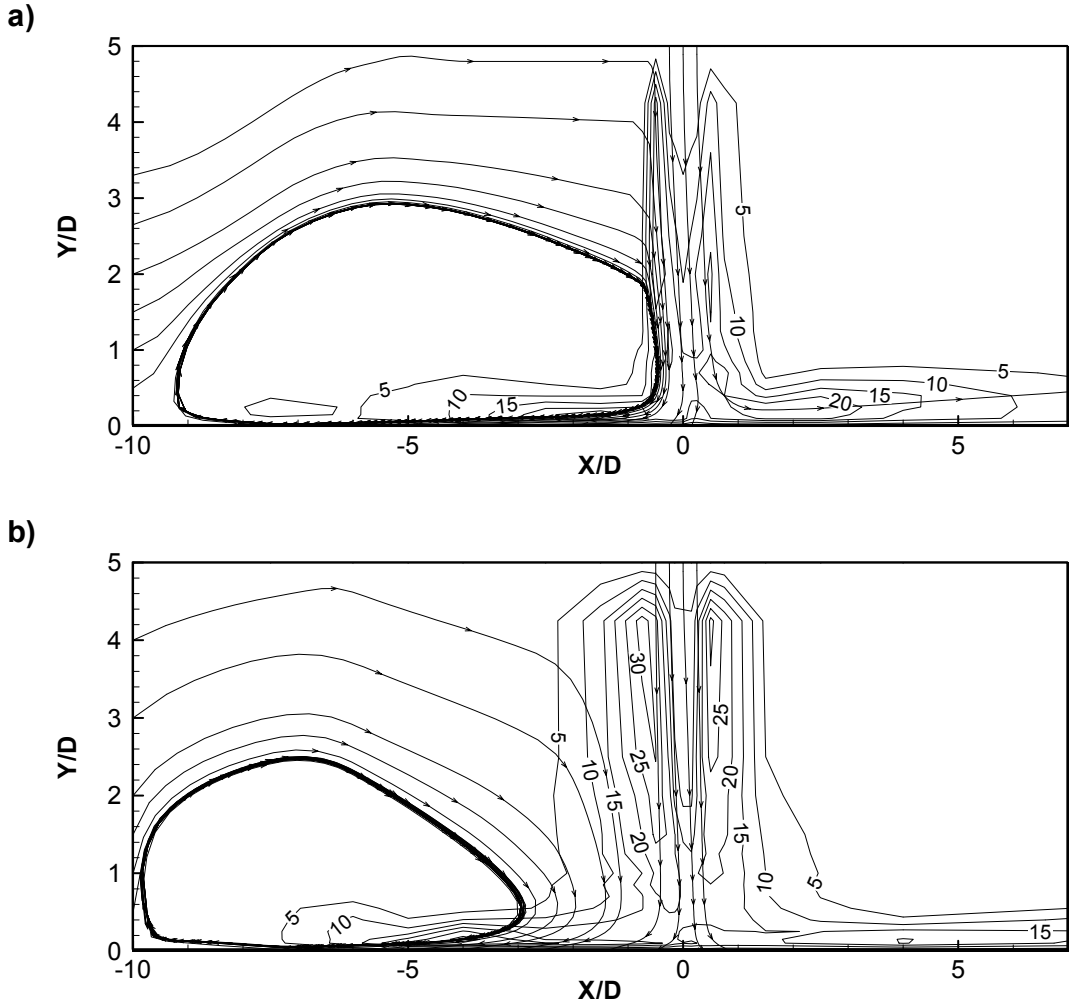

Fig. 5. Contours of measured horizontal velocity fluctuations u'^2x10^3/V_j^2 as a function of the jet-to-crossflow velocity ratio.
a) $V_j/U_o=30$
b) $V_j/U_o=45$

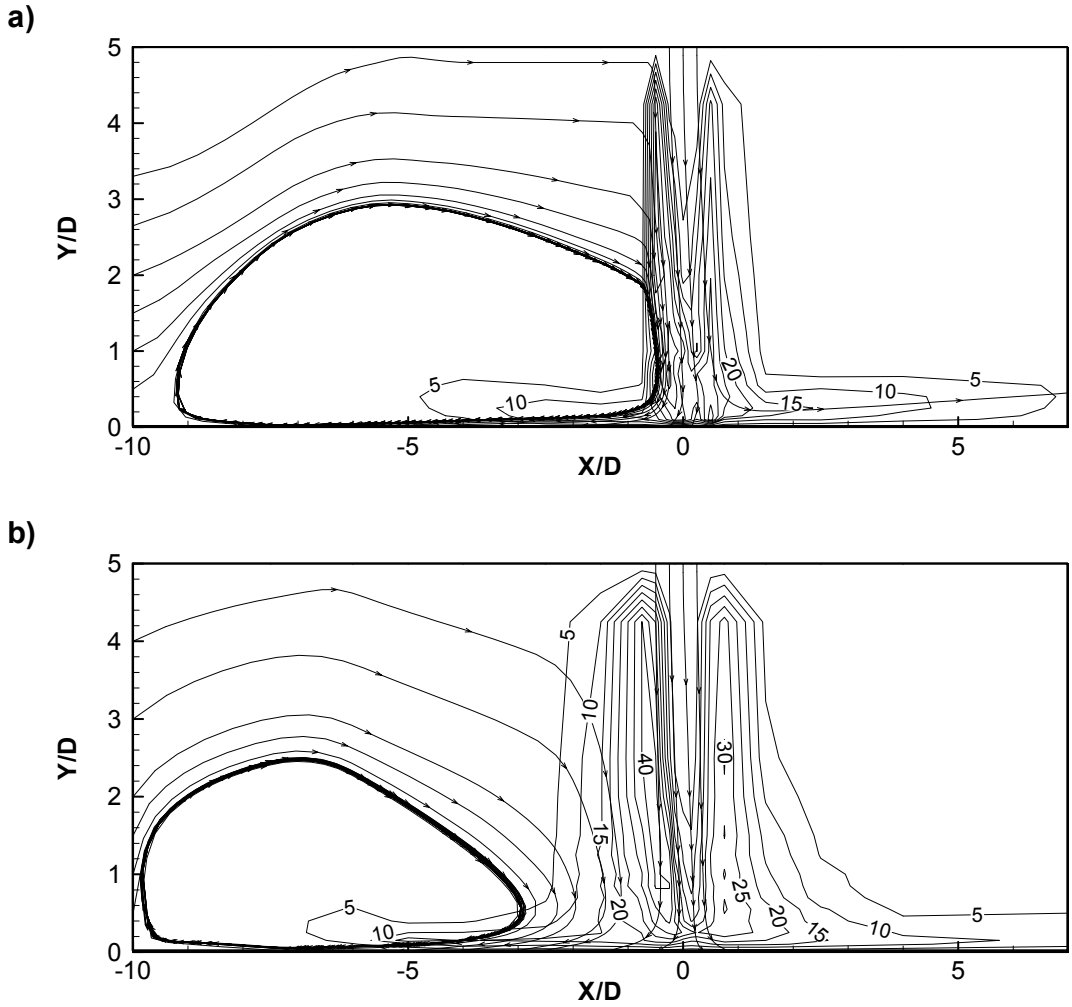

Fig. 6. Contours of measured vertical velocity fluctuations v'^2x10^3/V_j^2 as a function of the jet-to-crossflow velocity ratio.
a) $V_j/U_o=30$
b) $V_j/U_o=45$

4. DISCUSSION

The results of the previous section quantify the mean and turbulent velocity fields typical of impinging jets through a low-velocity crossflow and revealed the existence of two different flow regimes. One is characterized by larger flow asymmetries and ground vortex dimension with a large interference in the impinging zone and downstream flow development. Another corresponds to a symmetric impinging jet with a smaller ground vortex detached upstream with different implications on the downstream flow characteristics. The complex nature of the ground vortex and its implications on the turbulent structure of the impinging zone and of the far field makes it of utmost importance for a better understanding of this type of flows. Barata et al. (1989) and Barata (1993) had already identified some characteristics of the high velocity ratio impinging jet that causes many difficulties for the prediction of this type of flows. Knowles and Bray (1991) confirmed the complex nature of the flow and confirmed the need of better to understand the ground vortex. They demonstrated that much parametric work can be presented in terms of vortex penetration as a function of one of several parameters related with the ground pressure distribution (see figure 8). Vortex penetration can be quantified by using X_P, where the maximum static pressure occurs, or X_S, corresponding to the zero C_P. The most forward influence of the vortex is given by X_P and it has been used to quantify penetration. Another reason for its use is that smoke visualization gives a penetration that is close to that position. On the other hand, oil film flow visualization will tend to show the separation X_S, which is also more readily determined from ground pressure

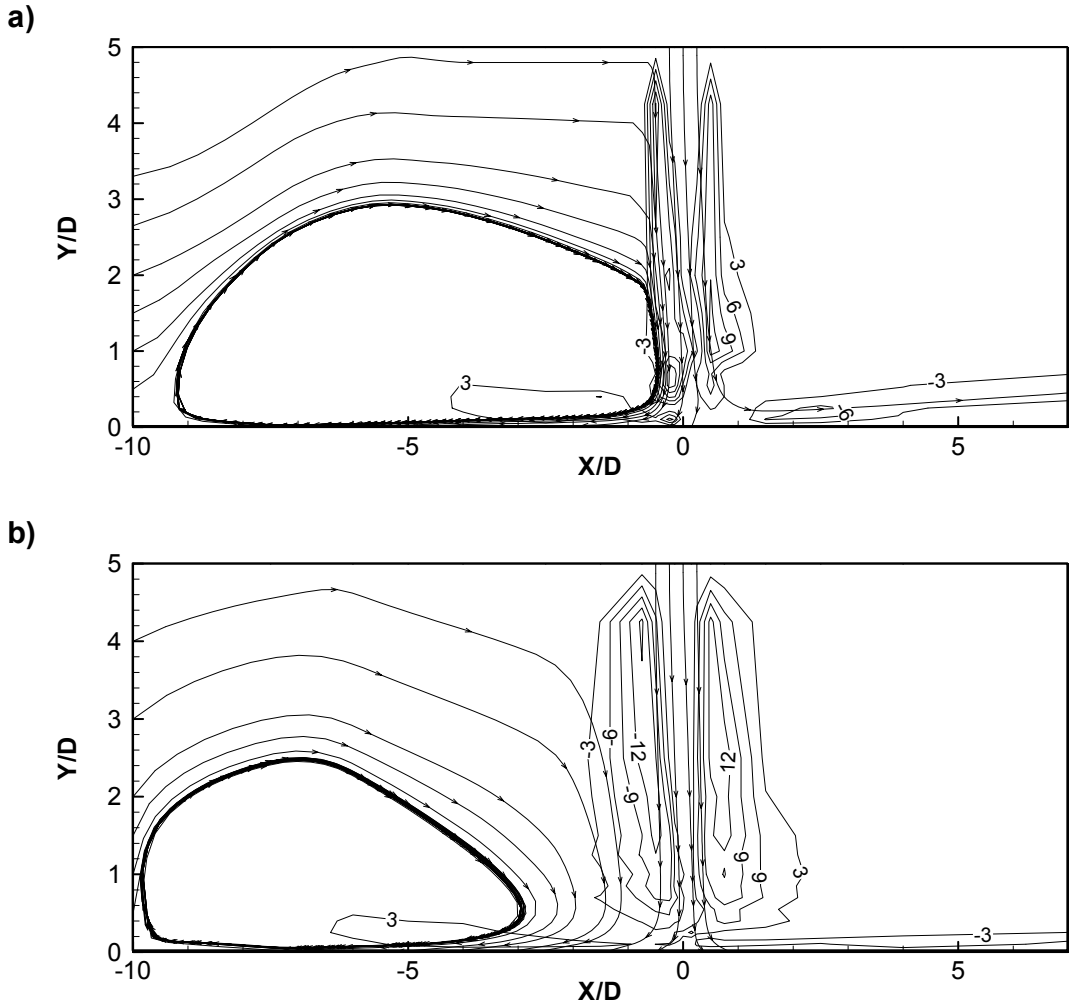

Fig. 7. Contours of measured Reynolds shear stress $u'v'x10^3/V_j^2$ as a function of the jet-to-crossflow velocity ratio.
a) V_j/U_o=30
b) V_j/U_o=45

distributions, due to the shallow curvature which is found near X_P. Similar parameters can be obtained from the velocity field that give some additional two- and three-dimensional information.

For example, the size and the location of the center of the ground vortex may give information on the flow regime. Results of figure 3 have shown that the center of the ground vortex is located at X/D=-5.6 for V_j/U_o=30 and at X/D=-7.2 for V_j/U_o=45, while the vertical coordinate of the center of the vortex is about Y/D=1.08 for the two velocity ratios. Nevertheless, the size of the vortex is reduced when V_j/U_o increases: the length is 8.8D for V_j/U_o=30 and 7.1D for V_j/U_o=45, while the height (H_v) is 2.95D and 2.55D, respectively. Figure 9 shows vertical profiles of the mean horizontal velocity component at the position of the center of the ground vortex for different velocity ratios. The profiles exhibit some similarity and confirm the vertical location of the center of the ground vortex. This figure also reveals that the increase in the crossflow velocity depends on the jet exit velocity. Taking into account only the blockage effect produced by the ground vortex, the crossflow velocity in the upper side of the channel would be 0.244m/s and 0.184m/s for the jet-to-crossflow velocities of 30 and 45, respectively. The measured values are considerable higher (0.336m/s and 0.378 m/s, respectively) because the ground vortex which is rotating in the clockwise direction induces an additional increase of the horizontal velocity. On the other hand, the strength of the ground vortex and this effect depends essentially on the jet exit velocity. It is interesting to note that for the velocity ratios considered the value of the crossflow velocity over the ground vortex is about V_j x U_o , which means that the smaller height of the ground vortex for higher velocity ratios is compensated by the increase of the vortex strength.

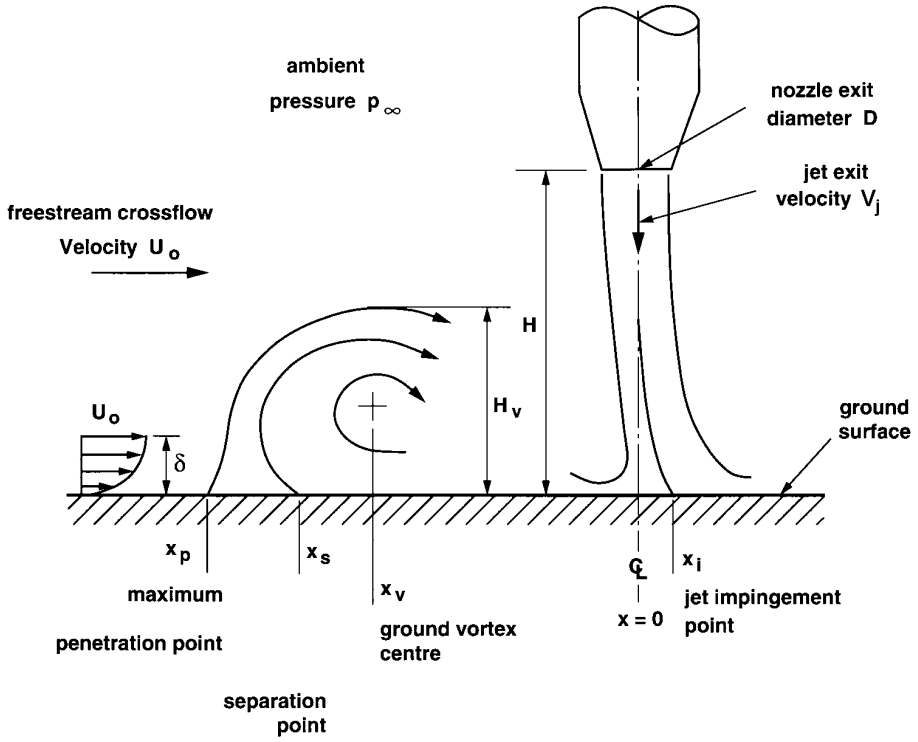

Fig. 8. Sketch of flow development in the plane of symmetry

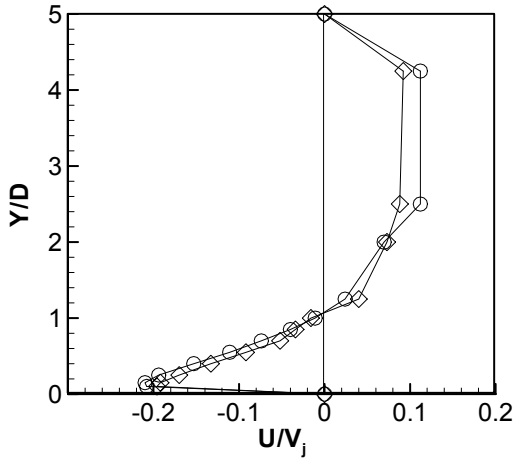

Fig. 9. Vertical profiles of the mean horizontal velocity at the location of the center of the ground vortex: O*, X/D=-5.6 for V_j/U_o =30; ◊, X/D=-7.2 for V_j/U_o=45.*

The effect of the jet-to-crossflow velocity ratio can be further characterized with the help of the horizontal profiles of the mean horizontal velocity component (U) shown in figure 10. The profile at Y/D=0.1 contains the maximum values of U along the wall jets (see also figure 4a) and show the initial development of the wall jets. Near the stagnation point, where the viscous effects are negligible, the mean horizontal velocity component increases linearly with X and then decays for the two velocity ratios, as expected. Nevertheless the two flow regimes already mentioned before can also be identified by the asymmetry of the profile for the smaller velocity ratio. The maximum values observed are $-0.55V_j$ and $+0.7V_j$ at X/D=-0.6 and X/D=+1.2, respectively, for V_j/U_o=30, while the same maximum absolute values ($0.7V_j$) are registered upstream and downstream at symmetric positions (X/D=±2.8) for V_j/U_o=45. This result is also associated with the position of the ground vortex whose downstream edge is located at the same position of the negative peak of U, i.e., at X/D=-0.6 and

X/D=-2.8 for V_j/U_o=30 and 45, respectively. The zero values far upstream the impinging zone indicate the separation point (X_S) that are located at X/D=–9.24 and X/D=–9.81 , which gives a ground vortex maximum length of L_V=8.8D and 7.1D for V_j/U_o=30 and 45, respectively. The horizontal profiles in the upper part of the wall jets at X/D=0.3 show directly the influence of the ground vortex on the impinging zone by the near zero values at X/D=-9.5 and -1.8 for V_j/U_o=30, and X/D=-9.8 and -2 for V_j/U_o=45, respectively. The profiles obtained at Y/D=1 cross the center of the ground vortex and are amplified in figure 10b. The peaks in the values of U are followed by near zero or negative horizontal velocities revealing the existence of a recirculation zone formed just downstream of the impinging jet by the deflection of the crossflow by the impinging jet.

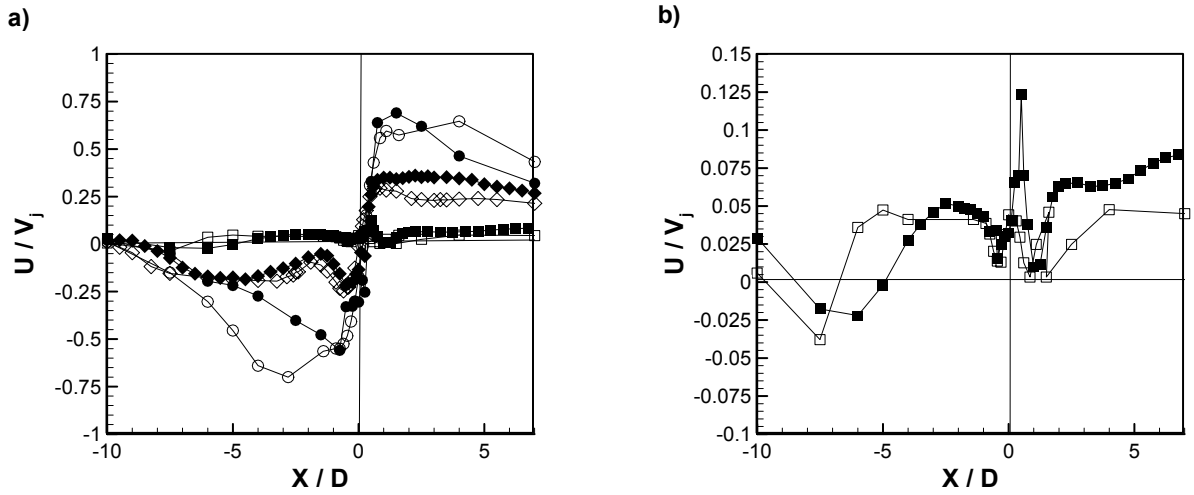

Fig. 10. Horizontal profiles of the mean horizontal velocity: O*, Y/D=0.1;* ◊*, Y/D=0.3;* □*, Y/D=1. (Key: closed symbols - V_j/U_o=30; open symbols - V_j/U_o=45).*

5. CONCLUSIONS

The flowfield resulting from the impingement of a single axisymmetric jet against a wall after penetrating a confined cross-flow has been studied experimentally using laser-Doppler anemometry. For sufficiently high jet velocities and small distances between the jet exit and the ground plane to produce impingement, two regions of the flow are seen to be of particular interest: the impinging region and the ground vortex due to the interaction between the upstream wall jet and the crossflow. The latter consists of a vortical structure that wraps around the impinging jet like a scarf and should develop further downstream through a pair of streamwise vortices.

The present work reports a study aimed at characterizing the influence of the jet-to-crossflow velocity ratio on the structure of the ground vortex. The experiments were performed for Reynolds based on the jet-exit conditions of between 60,000 and 105,000 corresponding to jet-to-crossflow velocity ratios from 30 to 73 and for an impinging height of 5 jet diameters, and two different regimes were identified. The first is characterized by the "contact" between the ground vortex and the impinging jet, while in the second the vortex is detached upstream the impinging zone.

The shape, size and location of the ground vortex were found to be dependent on the velocity ratio. A methodology based on the velocity measurements was developed to characterize the ground vortex. For the higher velocity ratio regime the downstream wall jet it is not strongly affected by the ground vortex, and the velocity profiles become similar. In both regimes, the crossflow acceleration over the ground vortex was found to be directly connected with the jet exit velocity. This indicates that the influence of the upstream wall jet is not confined to the ground vortex but spreads up to the upper wall by a mechanism that needs further investigation.

REFERENCES

Andreopoulos, J. and Rodi, W. (1984). "Experimental Investigation of Jets in a Crossflow", *J. Fluid Mechanics*, Vol. 138, pp. 127.

Araújo, S.R.B., Durão, D.F.G. and Firmino, F.J.G. (1982). "Jets Impinging Normally and Obliquely to a Wall", AGARD CP 308, paper 5.

Baker, O.J. (1981). "The Turbulent Horseshoe Vortex", *J. Wind Engineering and Industrial Aerodynamics*, Vol. 6, pp. 9.

Barata, J.M.M., Durão, D.F.G. and McGuirk, J.J. (1989). "Numerical Study of Single Impinging Jets Through a Crossflow", *Journal of Aircraft,* Vol.26, No.11, pp. 1002-1008.

Barata, J.M.M. (1989). "Numerical and Experimental Study of Jets Impinging on Flat Surfaces Through a Crossflow", Ph.D. Thesis (in Portuguese), Instituto Superior Técnico, Technical Univ. of Lisbon, Lisbon, Portugal.

Barata, J.M.M., Durão, D.F.G., Heitor, M.V. and McGuirk, J.J. (1993). "On the Analysis of an Impinging Jet on Ground Effects", *Experiments in Fluids*, No.15, pp.117-129.

Barata, J.M.M. (1996). "Fountain Flows Produced by Multiple Impinging Jets in a Crossflow", *AIAA Journal*, Vol.34, No.12, pp.2523-2530.

Crabb, D., Durão, D.F.G. and Whitelaw, J.H. (1981). "A Round Jet Normal to a Crossflow", *J. Fluids Engng.,* Vol.113, pp. 142-153.

Durst, F., Melling, A. and Whitelaw, J.H. (1981). "*Principles and Practice of Laser-Doppler Anemometry*", 2nd ed., New York, Academic Press.

Kamotani, Y. and Greber, I. (1974). "Experiments on Confined Turbulent Jets in a Crossflow", NASA CR-2392.

Knowles, K. and Bray, D. (1991). "The Ground Vortex Formed by Impinging Jets in Crossflow", AIAA 29th Aerospace Sciences Meeting, AIAA Paper 91-0768, Reno, NV, Jan. 7-10.

Melling, A. and Whitelaw, J.H. (1975). "Turbulent Flow in a Rectangular Duct", *J. Fluid Mechanics*, Vol. 78, pp.285-315.

Rajaratnam, R. (1976). "Turbulent Jets", Dev. in Water Science, 5, Elsevier Scientific Pub. Co., New York.

Schetz, J.A., Jakubowsky, A.K. and Aoyagi, K. (1984). "Surface Pressures on a Flat Plate With Dual Jet Configurations", *Journal of Aircraft*, Vol.21, No.7, 1984, pp. 484-490.

Shayesteh, M.V. Shabaka, I.M.N.A. and Bradshaw, P. (1985). "Turbulent Structure of a Three-Dimensional Impinging Jet in a Crossflow", AIAA 23rd Aerospace Sciences Meeting, AIAA Paper 85-0044, Reno, NV, Jan. 14-17.

Stoy, R.C. and Ben-Haim, Y. (1973). "Turbulent Jets in a Confined Crossflow", *J. Fluids Engng.*, No.95, pp.551-556.

Sugiyama Y. and Usami, Y. (1979). "Experiments on the Flow in and Around Jets Directed Normal to a Crossflow", *Bulletin JSME*, No.22, pp. 1736-1745.

Yanta, W.J. and Smith, R.A. (1978). "Measurements of Turbulent Transport Properties with a Laser-Doppler Velocimeter", 11th Aerospace Sciences Meeting, AIAA Paper 73-0169, Washington.